

Monte-Carlo Tree Search with Neural Network Guidance for Lane-Free Autonomous Driving

Ioannis Peridis, Dimitrios Troullinos, Georgios Chalkiadakis, Pantelis Giankoulidis, Ioannis Papamichail, and Markos Papageorgiou

Technical University of Crete

{iperidis, dtroullinos, gchalkiadakis, pgiankoulidis, ipapamichail, mpapageorgiou}@tuc.gr

Abstract

Lane-free traffic environments allow vehicles to better harness the lateral capacity of the road without being restricted to lane-keeping, thereby increasing the traffic flow rates. As such, we have a distinct and more challenging setting for autonomous driving. In this work, we consider a Monte-Carlo Tree Search (MCTS) planning approach for single-agent autonomous driving in lane-free traffic, where the associated Markov Decision Process we formulate is influenced from existing approaches tied to reinforcement learning frameworks. In addition, MCTS is equipped with a pre-trained neural network (NN) that guides the selection phase. This procedure incorporates the predictive capabilities of NNs for a more informed tree search process under computational constraints. In our experimental evaluation, we consider metrics that address both safety (through collision rates) and efficacy (through measured speed). Then, we examine: (a) the influence of isotropic state information for vehicles in a lane-free environment, resulting in nudging behaviour—vehicles' policy reacts due to the presence of faster tailing ones, (b) the acceleration of performance for the NN-guided variant of MCTS, and (c) the trade-off between computational resources and solution quality.

1 Introduction

The technological progress in autonomous vehicles, introducing as it does fast and reliable observational and connectivity capabilities, gives rise to research endeavours that envision forthcoming traffic environments with full autonomy. Among these, *lane-free traffic* [24] is a recently introduced paradigm that lifts the requirement for lane-keeping behaviour. In this manner, vehicles can operate freely within the road boundaries, and better harness road capacity [24].

One of the investigated vehicle movement strategies puts forward a Markov Decision Process (MDP) [16] for a single-agent formulation attached to (deep) reinforcement learning algorithms. An important aspect in lane-free autonomous driving is the notion of *nudging*, meaning that vehicles can observe both front and back-located vehicles, and react accordingly (e.g., a vehicle making space to assist a faster tailing vehicle). This is implicitly incorporated in the MDP of [16], but its effect is not actually examined; whereas it is empirically found to greatly improve upon the resulting policy for other methods [24]. To the best of our knowledge, no work to date tackles planning-based policies in lane-free traffic.

Against this background, in this paper we propose a refined MDP that is better suited to planning approaches, and put forward a systematic investigation of the potential created by using the celebrated Monte-Carlo Tree Search (MCTS) planning method [3] for *lane-free autonomous driving*. Moreover, we provide the framework for the integration of neural networks (NNs) in MCTS planning in this domain. To this end, we incorporate prior knowledge in our MDP with NNs and properly calibrate them with respect to MCTS-generated data, building on well-established lines of work [18] that incorporate NNs with prior knowledge (e.g., an expert policy) in the design of MCTS planning approaches. This integration can reduce the necessity for extensive computational efforts, i.e., achieve the same solution quality much faster. To this end, we employ an NN-Guided MCTS method [18], with a leveraged NN trained via offline self-play simulations in lane-free environments, utilizing data produced by our MCTS algorithm. With this, we can effectively determine the acceleration benefit of NNs in lane-free traffic, and discuss the computational trade-offs when NNs are involved.

We provide a systematic experimental evaluation of the trade-offs between computational effort and solution quality for lane-free autonomous driving, with metrics that assess safety and speed preferences in a challenging environment. Our results show that isotropic state information has a great impact on the decision-making, specifically resulting in nudging behaviour for vehicles, and high performance in challenging, high density traffic scenarios. Additionally, the NN-guided MCTS, significantly speeds up the tree search process in lane-free traffic, allowing the algorithm to exploit prior knowledge of the NN and return more informed results in fewer iterations.

2 Background and Related Work

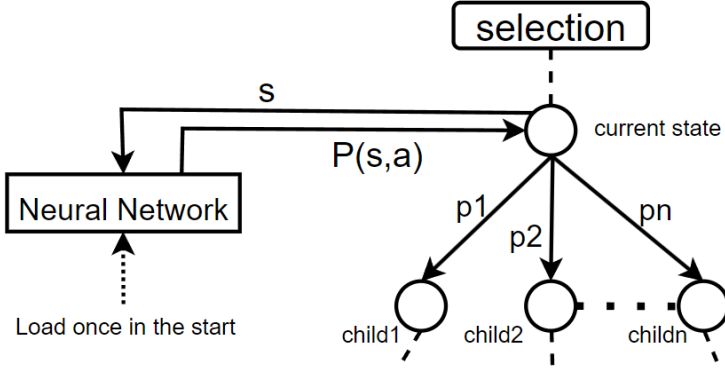
In this section, we introduce background information and discuss related work.

2.1 MDPs and MCTS with Neural Guidance

A Markov Decision Process (MDP) [2] models decision-making in stochastic sequential environments using a 5-tuple (S, A, P, R, γ) , where S is the state space, A is the action space, P is the transition probability, R is the reward function, and γ is the discount factor.

Monte-Carlo Tree Search (MCTS) [3, 29] is a solution method for MDPs based on planning, and it operates by simulating action paths to estimate long-term rewards, balancing exploration and exploitation. A search tree is built, using Monte-Carlo simulations to improve predictions. The tree expands iteratively through four phases—selection, expansion, simulation and backpropagation—emphasizing computational effort on promising areas of the decision space. For the selection phase, MCTS (typically) uses the Upper Confidence Bound for Trees (UCT) [20] formula, where a given a state s and a candidate action a at a tree node, the score is calculated as: $UCT(s, a) = Q(s, a) + C \sqrt{\frac{\ln N(s)}{N(s, a)}}$, where $Q(s, a)$ is the estimated expected average reward that is also updated iteratively according to the simulated outcomes, $N(s)$ is the state visit count, $N(s, a)$ is the action count, and C balances exploitation (optimize over the current estimate $Q(s, a)$) and exploration (expand the tree uniformly).

The embedding of deep learning into MCTS has been previously demonstrated in studies on Computer Go [18] and Hex [10]. These studies used neural networks (NNs) [12] to improve move prediction and evaluation by incorporating *neural guidance* into the selection phase of MCTS. NNs are typically pre-trained in a supervised manner from available datasets of expert players [18], which then can guide the planning tree. This training produces a model that predicts action probabilities from given states. Once trained, the NN guides MCTS in real-time, combining the prior knowledge of the NN with the dynamic search exploration of the MCTS.



$$\text{Select: } child_i = \underset{i \in \{1, 2, \dots, n\}}{\operatorname{argmax}} \{ PUCT_i \} = \underset{i \in \{1, 2, \dots, n\}}{\operatorname{argmax}} \{ UCT_i + f(p_i) \}$$

Figure 1: Illustration of NN-Guided selection, where the $child_i$ with the highest PUCT value is selected.

This is accomplished with PUCT [18, 10], an extension of UCT formula where selection can leverage the NN’s probability distribution $P(s, a)$ to evaluate action success, transforming the basic UCT search into a more sophisticated, *NN-guided* process. The PUCT formula, particularly variant 4 from [18], for a state s and action a is:

$$\text{score}(s, a) = Q(s, a) + C_b \cdot \sqrt{\frac{\ln N(s)}{N(s, a)}} + C_{pb} \cdot \frac{P(s, a)}{N(s, a) + 1} \quad (1)$$

where $P(s, a)$ is the NN-predicted probability of action a in state s , introducing neural guidance into MCTS. Parameters C_b and C_{pb} balance exploitation, exploration, and neural guidance. Figure 1 provides a visual illustration of Equation 1.

Integrating $P(s, a)$ into MCTS directs the search towards more promising actions. This leads to enhanced exploration efficiency, accelerates convergence to best strategies by quickly identifying promising policies, and requires less computational time. NN-Guided MCTS also improves decision quality under computational constraints, achieving high-quality decisions with fewer iterations or better solutions with the same number of iterations compared to plain MCTS. While NN-guided MCTS offers advantages, it also presents challenges, primarily due to the computational demands of NNs prediction. As mentioned in [10], this can cause an overhead that slows down the whole process, especially when dealing with deep architectures in real-time decision-making environments.

2.2 Related Work

MCTS methods, known for their incremental search capabilities, are applied in autonomous driving for simulating vehicle behavior considering human intentions [14], using KB-Trees [5], and employing probabilistic models to predict driver actions [22]. They are also used for maneuver prediction based on image inputs [4].

Lane-free traffic considers environments where vehicle movement strategies control vehicles without being restricted to lane-keeping. This transition to a more unstructured environment introduces complexities for motion planning, and requires innovative methods. The principal



Figure 2: Snapshot of the simulation environment.

work [24] that introduces the concept of lane-free traffic environments suggested heuristic rules to simulate “forces” for vehicle maneuvering, while [15] developed a cruise control system using Control Theory. Optimal control strategies using model predictive control were presented in [32], and [31] used the max-plus algorithm for multiagent decision making under a collaborative framework. Additionally, [16] developed an MDP framework for lane-free autonomous driving and applied it in a single-agent ring-road environment, using the Deep Deterministic Policy Gradient (DDPG) RL algorithm for policy optimization. Our MDP framework is highly influenced by that of [16] to apply MCTS in our autonomous lane-free driving environment.

3 Our Approach

In this section, we first present the lane-free traffic environment and the agent’s objectives, then define our MDP for MCTS in which our agent operates, and discuss aspects relevant to NN-Guided MCTS in lane-free traffic.

3.1 Lane-Free Traffic Environment

In this study, we model an open highway environment to simulate lane-free traffic scenarios with multiple automated vehicles, as shown in Figure 2. Each vehicle is an agent that observes its surrounding and has to update its action at every time-step, following an MDP formulation. Agents (vehicles) execute the MCTS algorithm independently, from their own local view, tackling the following two objectives, namely: follow a desired speed and avoid collisions. Each agent monitors its own longitudinal and lateral positions (p_x, p_y) and speeds (v_x, v_y) as well as the positions and speeds of nearby vehicles. All vehicles are standardized in size and movement dynamics, and each one possesses a *desired speed* sampled from a predefined range $[v_{d,\min}, v_{d,\max}]$. This represents the individual speed objective the agent wishes to reach and maintain. Control inputs for the agent include longitudinal and lateral accelerations (a_x, a_y), influencing gas/brake behaviour and left/right steering respectively.

For this lane-free traffic scenario, we use an extension of the Simulation of Urban MObility (SUMO) tool tailored for lane-free traffic [30]. The open highway environment is a straight road where vehicles constantly enter the highway’s entry point following a flow demand value, i.e., how many vehicles to be entered per hour, and then exit once they reach the end of the road.

3.2 State Space

Firstly, we define the state space \mathcal{S} . A vehicle c is characterized by attributes: $c = \{p_x, p_y, v_x, v_y, l, w, v_d\}$, where each attribute is defined as presented in Table 1.

At any moment t , the state of a vehicle c includes its own characteristics, along with information about nearby vehicles within a visibility distance d . A state s is described as $s = \{c_n, \Gamma = [c_1 \dots c_m]\}$, where c_n is the ego vehicle, and Γ is the set of neighboring vehicles located in front and behind the ego vehicle within a prescribed observational longitudinal distance. An instrumental aspect in approaches for lane-free traffic is *nudging*, that is, vehicles observe and react to nearby vehicles located on the back as well, instead of typical car-following behaviour where vehicles adjust their behaviour only according to leading vehicles. The related MDP formulation of [16] also incorporates such state representations with isotropic information regarding both leading and tailing vehicles. A terminal state is reached when the ego vehicle collides with another vehicle or exceeds the road boundaries.

3.3 Action Space

For constructing a search tree within our algorithm, the action space \mathcal{A} is discretized into a finite set of possible accelerations. An action α is defined as a pair of selected accelerations, $\alpha = \{a_x, a_y\}$, where a_x and a_y are chosen from predefined sets:

- Longitudinal acceleration values (m/s^2): $a_x = \{-5, -2, 0, 2, 5\}$
- Lateral acceleration values (m/s^2): $a_y = \{-1, 0, 1\}$

This discretization is visualized in Figure 3 and results in a set of 15 distinct actions, providing a manageable set of maneuvers to choose from.

3.4 Reward Function

The reward function guides the algorithm towards finding the optimal policy by quantifying the outcomes of different actions under various states. The primary goals are collision avoidance and maintaining a speed close to the *desired* one. Therefore, given a state s reached after the rollout, the reward to be backpropagated is calculated as follows.

3.4.1 Collision Avoidance Objective

For collision avoidance, we have a collision “negative reward” (penalty) term $r_c(s)$. If a collision occurs during rollout, the simulated state is terminal. The penalty is lower for collisions occurring later (deeper) in the simulation, as they are, intuitively, less likely to occur in practice. That is,

$$r_c(s) = \begin{cases} -\frac{D}{n_s}, & \text{in case of a collision occurrence} \\ 0, & \text{otherwise} \end{cases} \quad (2)$$

Parameter	Definition
p_x (m)	Position in x-axis
p_y (m)	Position in y-axis
v_x (m/s)	Speed in x-axis
v_y (m/s)	Speed in y-axis
l (m)	Vehicle length
w (m)	Vehicle width
v_d (m/s)	Desired speed

Table 1: Vehicle’s state information.

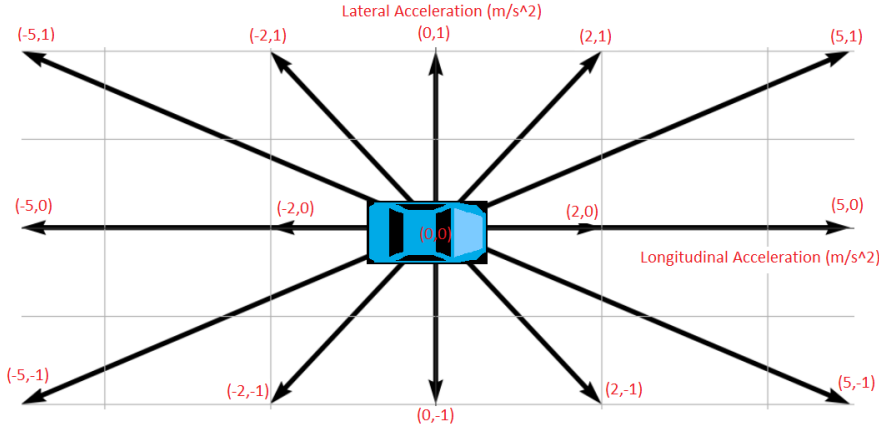


Figure 3: Action Space consists of 15 discrete actions in the 2-dimensional space $\{a_x, a_y\}$.

where D is a positive constant and n_s is the number of steps after the current state (i.e., the tree depth), as such calibrating the collision’s significance based on how far ahead in the simulation it occurs. If no collision occurs in the rollout, then $r_c(s)$ has no influence.

Additionally, artificial potential fields [16] measure collision risk based on relative positions and speeds between two vehicles i, j , calculated by the function f_{ij} . Besides adding a more informed element for proactive collision avoidance, they also promote safety-related gaps that the vehicles should adhere to. If $f_{ij} = 0$, then vehicles i, j already maintain proper distances, while for $f_{ij} < 0$, ego vehicle i should react accordingly. The use of fields—in conjunction with our state representation—additionally enables nudging behaviour, meaning that vehicles can react to faster tailing vehicles usually to give them space to overtake. A more detailed presentation can be found in [16]. As such, we also include a cumulative reward term $r_f(s)$ based on the influence of surrounding vehicles in the observed state. The related term is given by:

$$r_f(s) = \sum_{j=1}^{\Gamma} f_{ij} \cdot (dx_{ij} \leq d_{max}) \quad (3)$$

where Γ is the set of neighbors in state s , then dx_{ij} is the longitudinal distance between vehicles i and j , and d_{max} is an influence zone that prunes the effect of vehicles j that are located outside of the designated area.

3.4.2 Desired Speed Objective

For this, we focus on minimizing the distance between the vehicle’s speed v_x at state s and the desired speed v_d . The heuristic for the desired speed maintenance objective is defined as:

$$r_v(s) = \frac{\epsilon}{|v_x - v_d| + \epsilon} \quad (4)$$

where ϵ is a positive constant that avoids division with zero.

3.4.3 Objectives Integration

The total reward $r(s)$ for a simulation, considering both collision avoidance and speed maintenance, is calculated as a weighted sum:

$$r(s) = \begin{cases} \alpha \cdot r_f(s) + \beta \cdot r_c(s), & r_c(s) \neq 0 \\ \alpha \cdot r_f(s) + c \cdot r_v(s), & \text{otherwise} \end{cases} \quad (5)$$

where α, β, c are coefficients weighing the importance of the associated terms. Therefore, we always have the influence from the fields ($r_f(s)$), and select to either contain the collision-related reward ($r_c(s)$) or motivate the agent to pursue its desired speed ($r_v(s)$) if the situation does not result in a collision.

3.5 Simulation of Future States in Rollout Phase

The outcome of a vehicle's action within the simulation is deterministic. When a vehicle is in a particular state and takes an action, the next state is determined by the commonly used kinematic equations of the double integrator model. For the longitudinal axis (x), the equation for the speed update is: $v'_x = v_x + a_x T$. Then, the vehicle's updated position is calculated by: $p'_x = p_x + v_x T + \frac{1}{2} a_x T^2$, where p_x represents the position at current state s , v_x denotes the speed, a_x signifies the applied acceleration at that time-step, and T is the constant time-step duration. Likewise, the lateral axis (y) follows the same updates.

Therefore, when an action $a = \{a_x, a_y\}$ is executed, we can simulate the resulting state s' for the ego vehicle's information. However, we need to additionally simulate the neighboring vehicles' state information. To do so, we assume that they perform a "neutral" action—that is, zero acceleration on both axes $a = \{0, 0\}$. Thus, their speeds remain unchanged for the simulation purposes, and their positions are updated using the same kinematic equation: $p'_x = p_x + v_x T$. The simulation outcomes, with scores calculated from reward function $r(s)$, provide valuable information for evaluating the simulated states.

3.6 NN Pre-Training and Calibration

To construct a dataset for learning purposes, we collect data through "self-play" simulations using the standard MCTS algorithm. This dataset includes inputs (states) and corresponding labels (actions determined by MCTS), where each input element has a vector form of fixed size for compliance with the NN. After training, if we directly evaluate the calibration on a validation dataset, we obtain a low 72% score for accuracy, even after empirical fine-tuning of the NN architecture and training-related parameters. However, this was to be expected, since we (naively) employed this metric instead of addressing the inherent probabilistic nature of the collected MCTS data. As such, we instead evaluate the trained NN with the use of tools that better capture the accuracy of NNs trained from probabilistic data. To this end, we employ *Reliability Diagrams* [13], and partition the dataset into 10 bins for evaluation based on the probability of the action taken. As shown in Figure 4, when we examine the partitioned space, our model closely aligns with the "ideal" calibration, indicating that the trained NN is quite adept. More details regarding relevant background, data collection and evaluation process, and other technical information can be found in the Appendix Section A.

3.7 Technical Aspects of NN integration into MCTS

As discussed in [10], a practical limitation of incorporating NN predictions is the computational overhead of the online forward pass for predictions. Authors briefly mentioned that they resorted

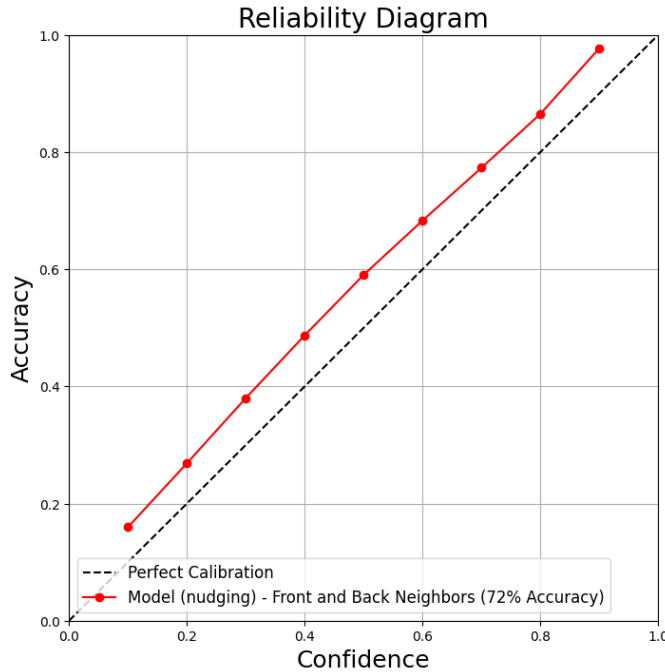


Figure 4: Reliability Diagram of trained NN’s calibration compared to a perfect calibration plotted line.

to an asynchronous technique to pipeline the procedure. In this work, while we are more inclined towards the investigation of the acceleration benefits and impact of the NN-guided MCTS in our domain, we have already done some groundwork to improve upon actual execution times. After early attempts based on memoization for $P(s, a)$ on each tree node, we harness the parallelization capabilities of a GPU through preemptive *batch predictions* for child nodes (at the root tree state before the initiation of MCTS) up to a prespecified tree-depth, and therefore have the information for $P(s, a)$ readily available. More details can be found in the Appendix Sections B, C.

4 Experimental Evaluation

This section details our environment setup and simulation parameters. We compare the performance of four algorithms: plain MCTS, MCTS enhanced with nudging, NN-Guided MCTS, and standalone NN, across various scenarios to evaluate their effectiveness.

Table 2 summarizes the parameters of our lane-free simulation environment. Other parameter settings can be found in Appendix Section C.

4.1 Algorithms, Metrics, Environment and MCTS Settings

4.1.1 Examined Algorithms

Our experiments evaluate several variants. *MCTS* is a basic implementation where the ego vehicle is aware of only the vehicles in front. *MCTS (nudging)* enhances the state information about vehicles behind the ego vehicle, improving state awareness and resulting in nudging behaviour

Parameter	Value
Simulation Time (sec)	3600
Simulation Time-Step (sec)	0.25
Vehicle Length (m)	3.5
Vehicle Width (m)	1.6
Demand flow (veh/h)	5400, 9400, 12000
Departure Speed (m/s)	25
Desired Speed (m/s)	[25, 35]
Road Length (m)	500
Road Width (m)	10.2

Table 2: Simulation Parameters.

that significantly improves upon the resulting policy, as also suggested in other studies [24]. *NN-MCTS* combines NN predictions with *MCTS (nudging)* for data-driven guidance. Lastly, *NN* is the straightforward NN approach without any search methods, used to evaluate its standalone decision-making efficacy.

4.1.2 Assessed Metrics

The performance of our algorithms is assessed using two key metrics. Collisions count the total incidents where two vehicles collide with each other, with fewer collisions indicating better decision-making. Speed Average calculates the mean speed of all vehicles, ideally close to 30m/s (due to ranging from 25 to 35m/s), reflecting the algorithm’s efficiency in maintaining a relatively high speed.

4.1.3 Examined Flow Demands on Open Highway

Our algorithms are tested across ranging vehicle flow levels on an open highway to assess their performance under increasingly challenging scenarios. As vehicle flow per hour rises, traffic density increases, complicating decision-making and necessitating more delicate maneuvers to avoid collisions. Higher traffic density typically reduces average speed, and sometimes can lead to unavoidable collisions for policies that under-perform. We evaluate our agents under three flow rates: 5400 *veh/h* (low traffic), 9400 *veh/h* (intermediate traffic), and 12000 *veh/h* (high traffic), each testing the algorithms’ ability to maintain efficiency and safety in progressively denser conditions.

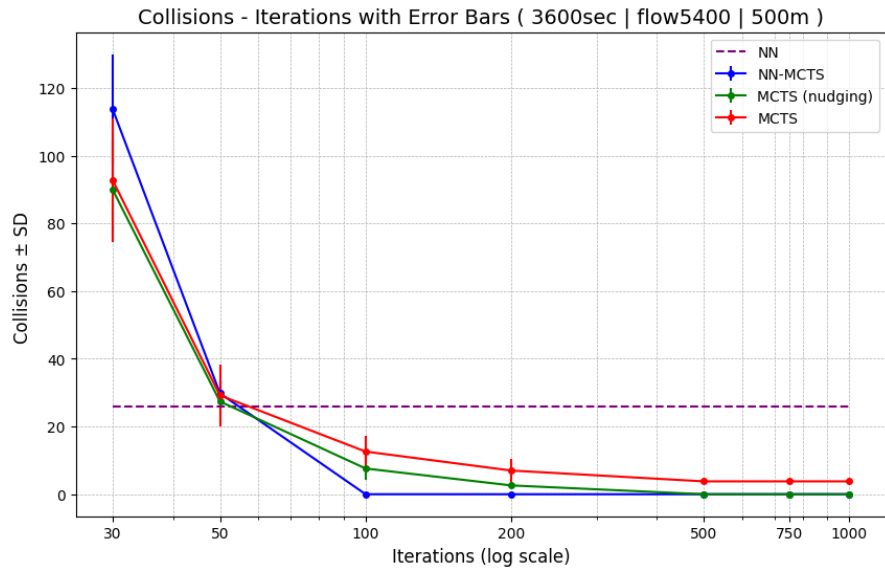


Figure 5: Graph of Collisions \pm SD for NN-MCTS, MCTS (nudging), MCTS and NN across different Iterations for 5400 *veh/h*.

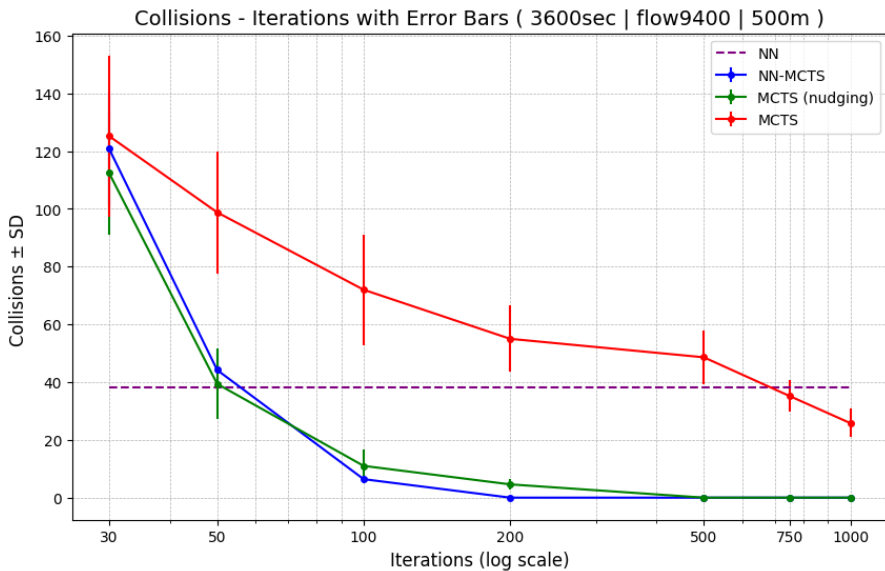


Figure 6: Graph of Collisions \pm SD for NN-MCTS, MCTS (nudging), MCTS and NN across different Iterations for 9400 *veh/h*.

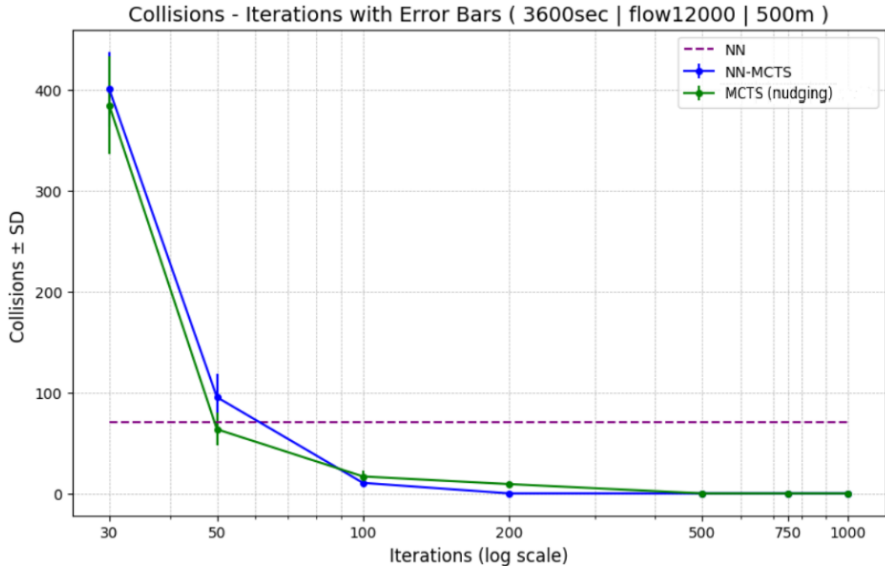


Figure 7: Graph of Collisions \pm SD for NN-MCTS, MCTS (nudging), MCTS and NN across different Iterations for 12000 veh/h .

4.1.4 MCTS Iterations

In our experimental setup, we vary the number of MCTS iterations for each algorithm, ranging from 30 to 1000, to evaluate their performance under different computational constraints. This approach helps identify the efficiency of each algorithm in finding best actions with minimal iterations. The goal is to determine the convergence point, where performance peaks and additional iterations yield no notable improvement in result quality. By comparing how quickly each algorithm reaches this point and the quality of their results at convergence, we can assess their computational efficiency and efficiency of decision-making. All results are averaged from 5 different seeds.

4.2 Collisions Avoidance Results

In Figures 5–7, we present the collisions-iterations diagrams for each demand flow, where accompanying tables detailing the average of collisions and their \pm standard deviations for all algorithms across different iteration samples can be found in the Appendix Section D. We use a logarithmic scale for the iterations axis in our graphs to emphasize performance improvements at lower iteration counts, where significant changes occur, while higher iterations exhibit minimal variation. From all figures above, we observe that each MCTS algorithm starts with high collision counts, which decrease as iterations increase, indicating more effective decision-making with deeper state exploration.

4.2.1 Comparison: MCTS vs MCTS (nudging)

Our comparative analysis shows that MCTS (nudging) consistently outperforms MCTS in reducing collisions across all vehicle flows. MCTS (nudging) achieves stabilization with zero collisions at 500 iterations for all tested flows, whereas MCTS struggles to reach the best performance, particularly at higher flows. At 12000 veh/h , MCTS is completely incompetent without nudging,

resulting in collisions that prevent the simulation from proceeding. Additionally, MCTS shows larger standard deviations (error bars), indicating less reliable performance. These findings demonstrate that MCTS (nudging), just with its enhanced visibility of back neighbors, makes use of the additional information and substantially improves the resulting policy (with nudging effect).

4.2.2 Comparison: MCTS (nudging) vs NN-MCTS

NN-MCTS significantly outperforms MCTS (nudging) in reducing collisions more efficiently across all vehicle flows. NN-MCTS achieves zero collisions with far fewer iterations: only 100 iterations at a 5400 veh/h flow, compared to MCTS (nudging), which requires 500 iterations (400 fewer). At higher flows of 9400 and 12000 veh/h , we observe the same phenomenon but naturally requiring more iterations as the problem is more complex. When NN-MCTS converges first, MCTS (nudging) still experiences collisions, indicating that NN-MCTS's early stabilization marks a phase where plain MCTS is yet to optimize fully and returns inferior results. These findings highlight the accelerated efficiency of NN-MCTS due to the impact of leveraging the NN's predictive capabilities. Notably, at lower iterations (30 and 50), plain MCTS performs slightly better than NN-MCTS. We attribute this to the initial biases introduced by the NN in NN-MCTS, as the NN is trained on simulations running at 1000 iterations, meaning that its guidance is optimized for longer search processes. The early termination prevents NN-MCTS from fully utilizing its pre-trained knowledge, making it more affected by early cutoffs.

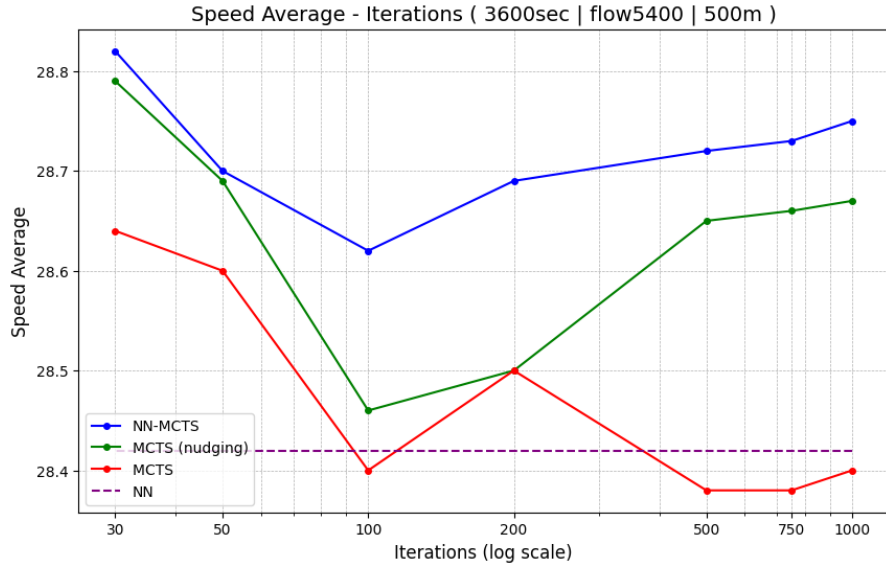


Figure 8: Graph of Speed Average \pm SD for NN-MCTS, MCTS (nudging), MCTS and NN across different Iterations for 5400 veh/h .

4.2.3 NN Performance and Comparisons

The simple NN, which naively predicts the next action, is depicted with a straight-line in graphs as it does not involve iterative computations. It only outperforms other algorithms at low iteration counts as these algorithms have not had enough iterations to optimize their solutions. However, as the iteration count increases other algorithms delve deeper and yield more informed

solutions. Naturally, this is due to the NN's greedy approach, which follows a deterministic strategy without exploring alternative paths. Despite being trained on data from MCTS (nudging) the NN does not replicate expected outcomes due to training inaccuracies and inherent randomness in MCTS data.

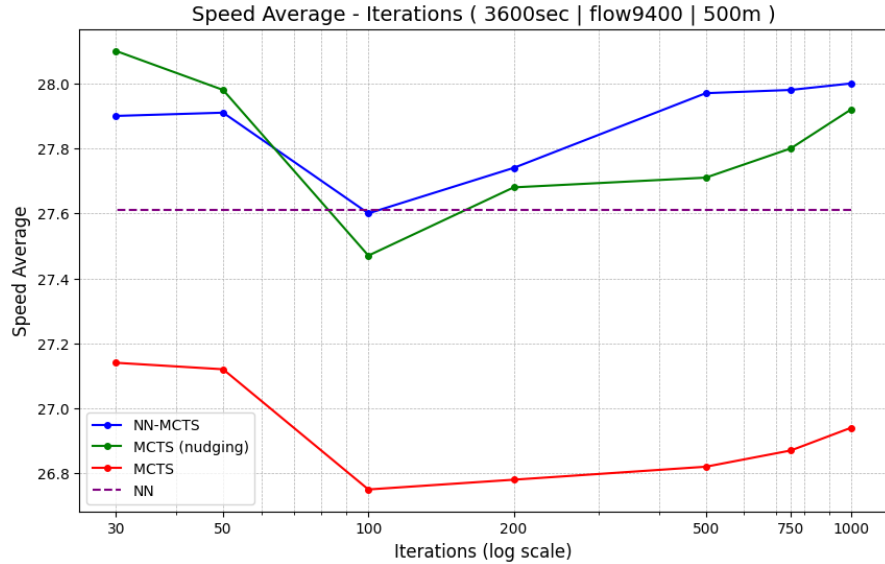


Figure 9: Graph of Speed Average \pm SD for NN-MCTS, MCTS (nudging), MCTS and NN across different Iterations for 9400 *veh/h*.

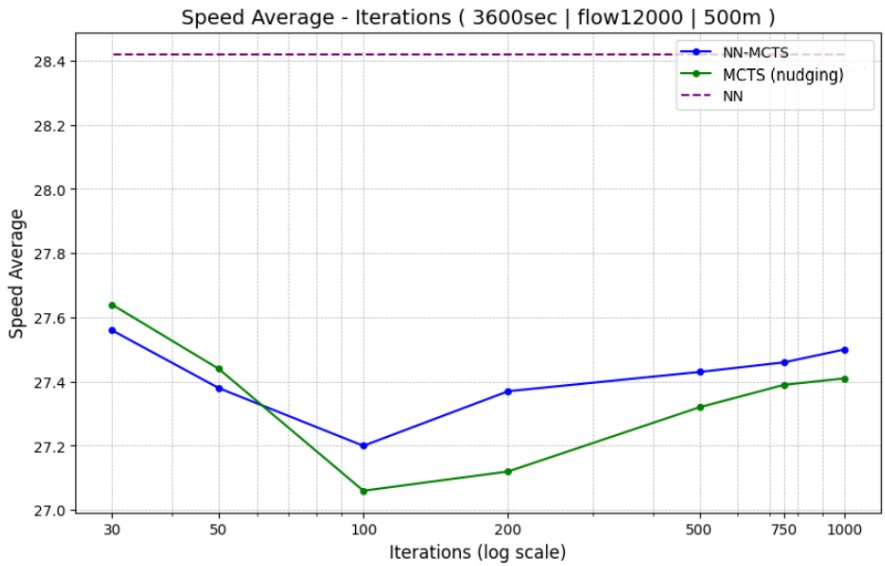


Figure 10: Graph of Speed Average \pm SD for NN-MCTS, MCTS (nudging), MCTS and NN across different Iterations for 12000 *veh/h*.



Figure 11: Initial conditions of the example.

4.3 Average Speed Results

Following our discussion, we present the figures for average speed-iterations across all vehicle flows in Figures 8–10. As vehicle flow increases, MCTS-based algorithms show decreased average speeds. This trend highlights the impact of higher traffic density, necessitating more cautious driving behaviors to avoid collisions, which results in slower traffic movement and longer delays. Complementary results are available in the Appendix Section D.

The analysis of speed metric aligns with our previous findings from collision results. MCTS (nudging) consistently outperforms MCTS across all vehicle flows, demonstrating better average speeds, particularly at higher densities where MCTS fails to execute effectively. NN-MCTS marginally surpasses MCTS (nudging), showing slight improvements once stabilized, although these enhancements are not as substantial. A related observation is that we do not have convergence for the speed metric, i.e., it is marginally improved even when we reach our imposed limit of 1000 iterations. Additionally, in contrast to the collision-related results, the standard deviation (error bars) is consistently close to 0 for all algorithms. The plain NN, while consistently worse than both NN-MCTS and MCTS (nudging), still performs better than MCTS in most scenarios, further illustrating the limitations of MCTS without the nudging effect. Overall, the findings confirm that the improvements observed in collision metrics also apply to speed, reaffirming the superior performance of MCTS (nudging) and NN-MCTS.

At lower iteration counts (30 and 50), a slight improvement in speed average is observed across all algorithms. This improvement is due to the algorithms not yet stabilizing their decision-making processes, resulting in more “reckless” decisions that lead to higher speeds. However, these decisions are not sustainable or safe, as evident by the associated collisions. The vehicles exhibit behaviors such as lack of proper nudging, and non-compliance with safety rules, contributing to short-term improvements in speed but at the cost of increased risk and collisions.

4.4 Simulation Execution Example and Vehicle Trajectories

In this section, we demonstrate the resulting behaviour of the NN-Guided MCTS through the trajectories of the video example found in the supplementary material. In this example, the vehicles operate with different desired speeds, namely 29, 32, and 34m/s. The initial conditions of the scenario are shown in Figure 11, with the blue vehicles being the ones we focus at. The provided figures provide a clear visualization of the trajectories for position and speed of the vehicles as they evolve over time in the simulation, with the x axis containing the discrete time-steps.

Vehicle Trajectories: Lateral Position p_y (m) – Time (time-steps) Figure 12 shows the lateral positions of the vehicles, mapping their trajectories across the road’s width. Rising curves indicate left turns, falling curves indicate right turns, and flat lines show straight movement.

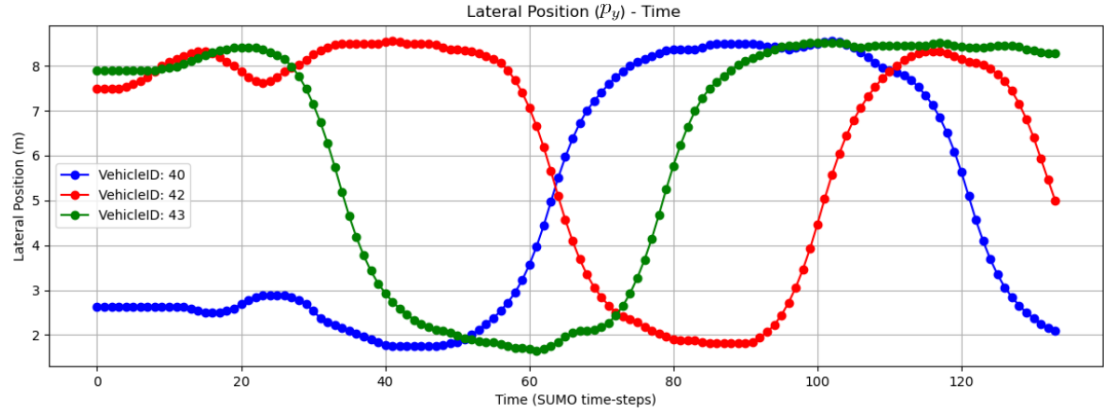


Figure 12: Lateral position p_y (m) – Time (time-steps) for vehicles with IDs 40, 42 and 43 from the simulation.

The figure above aligns with the trajectories observed in the simulation video, showcasing the NN-Guided MCTS algorithm’s effectiveness. The vehicles not only accelerate to achieve their desired speeds but also perform complex maneuvers and efficiently navigate between other vehicles, maintaining safe distances to avoid collisions.

Vehicle Speed: Longitudinal Speed v_x (m/s) – Time (time-steps) Figure 13 depicts the longitudinal speeds. Upward trends signify acceleration, while downward trends indicate deceleration along the x-axis.

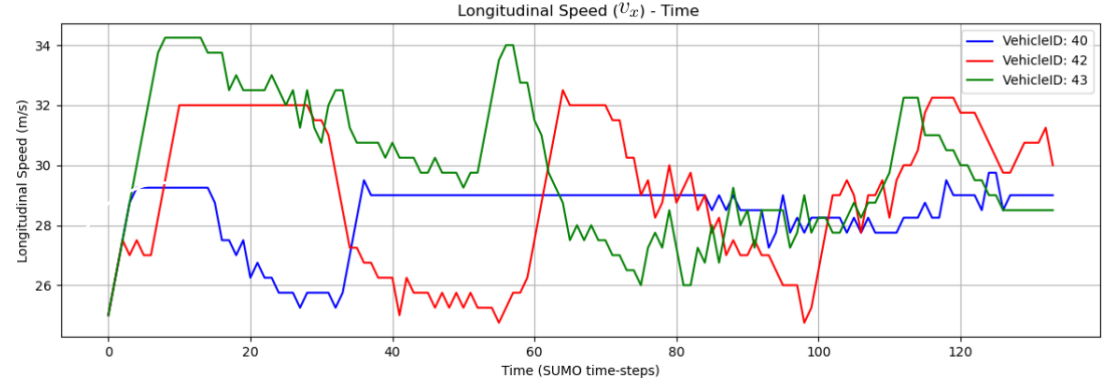


Figure 13: Longitudinal speed v_x (m/s) – Time (time-steps) for vehicles with IDs 40, 42 and 43 from the simulation.

The figure above also highlights the variance in vehicle speeds relative to their desired targets. For instance, vehicle 40, with a desired speed of $29m/s$, maintains lower speeds, while vehicle 43, aiming for $34m/s$, reaches the highest speeds. This indicates that each vehicle actively tries to match its target speed, with adjustments for braking and maneuvers to avoid collisions.

Lateral speed v_y (m/s) – Time (time-steps) Figure 14 visualizes lateral speeds, where positive values indicate leftward movement, and negative values signify rightward movement.

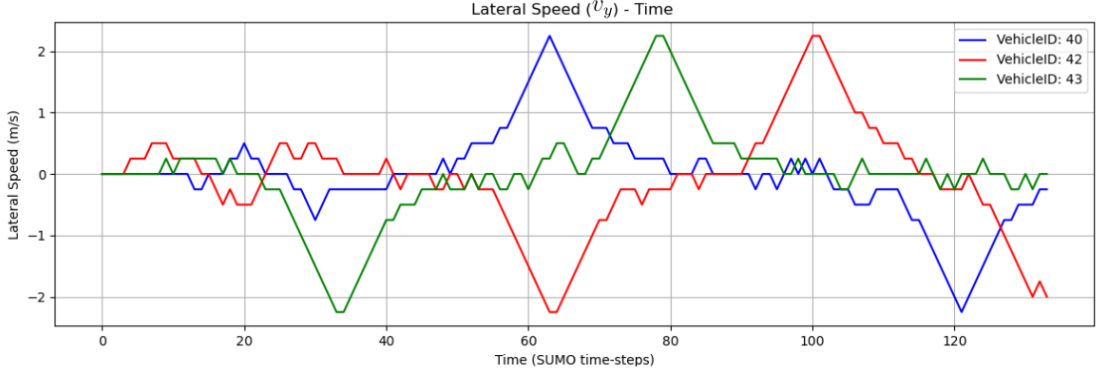


Figure 14: Lateral Speed v_y (m/s) – Time (time-steps) for vehicles with ID’s 40, 42 and 43 from the simulation.

Furthermore, the figure above shows the relationship between lateral speed changes and vehicle positioning. Smaller variations result in minor trajectory shifts, whereas larger changes lead to more distinct movements. These observations exhibit the algorithm’s ability to adapt to dynamic driving conditions.

5 Conclusions and Future Work

In this paper, we developed an MDP for an MCTS algorithm in lane-free traffic environments, and examined the influence of backward state awareness in nudging behaviour. We further integrated a neural network into the MCTS selection phase, trained through self-play simulations to provide predictive guidance. Especially in scenarios with limited iterations, our experimental evaluation shows that integrating NN guidance to MCTS enhanced with nudging, can deliver more sophisticated and better informed results, as plain MCTS may not be able to find the solutions of high quality under a designated (realistic) time allowance.

In future work, we can examine neural guidance in other MCTS phases [18, 9, 28], a guided expansion mechanism within MCTS could enable more sophisticated decisions. By selectively expanding only those child nodes identified as promising by the NN and pruning the others, we can efficiently manage increased action space complexity. In relation to that, extending NN guidance into the simulation phase of MCTS [18, 27] can improve the predictive accuracy of simulations. In our domain, this involves simulating neighbor vehicle actions based on the NN’s learned policy, resulting in more accurate and strategic simulations. Moreover, shifting from offline supervised learning to an online learning paradigm [18, 6, 25] is another potential avenue. These dynamic, iterative approaches, involve continuous policy improvement via MCTS during the actual tree search process, creating a feedback loop between MCTS and the NN. Additionally, extensions that address Continuous action spaces for MCTS [21, 19, 33] would fare favourably in our inherently continuous lane-free environment domain.

Finally, NN-MCTS has a time overhead due to the combined use of Python for NN predictions and C++ for the MCTS search procedure through Pybind11, therefore not currently representative of the execution time of proper native implementation that would have to be employed in

a real-time system. To this end, technical developments towards a native C++ solution (instead of the current hybrid C++/Python environment), combined with the existing practical choices (e.g., batch prediction) would make future approaches much faster in terms of execution times and therefore better conforming to realistic time constraints.

Acknowledgements

The research leading to these results has received funding from the European Research Council under the European Union’s Horizon 2020 Research and Innovation programme/ERC Grant Agreement n.[833915], project TrafficFluid.

References

- [1] M. Abadi, A. Agarwal, P. Barham, E. Brevdo, Z. Chen, C. Citro, G. S. Corrado, A. Davis, J. Dean, M. Devin, S. Ghemawat, I. Goodfellow, A. Harp, G. Irving, M. Isard, Y. Jia, R. Jozefowicz, L. Kaiser, M. Kudlur, J. Levenberg, D. Mané, R. Monga, S. Moore, D. Murray, C. Olah, M. Schuster, J. Shlens, B. Steiner, I. Sutskever, K. Talwar, P. Tucker, V. Vanhoucke, V. Vasudevan, F. Viégas, O. Vinyals, P. Warden, M. Wattenberg, M. Wicke, Y. Yu, and X. Zheng. TensorFlow: Large-scale machine learning on heterogeneous systems, 2015. Software available from tensorflow.org.
- [2] R. Bellman. A markovian decision process. *Journal of Mathematics and Mechanics*, pages 679–684, 1957.
- [3] C. Browne, E. Powley, D. Whitehouse, S. Lucas, P. Cowling, P. Rohlfshagen, S. Tavener, D. Perez Liebana, S. Samothrakis, and S. Colton. A survey of monte carlo tree search methods. *IEEE Transactions on Computational Intelligence and AI in Games*, 4(1):1–43, Mar 2012.
- [4] N. Catenacci Volpi, Y. Wu, and D. Ognibene. Towards event-based mcts for autonomous cars. In *2017 Asia-Pacific Signal and Information Processing Association Annual Summit and Conference (APSIPA ASC)*, pages 420–427. IEEE, 2017.
- [5] J. Chen, C. Zhang, J. Luo, J. Xie, and Y. Wan. Driving maneuvers prediction based autonomous driving control by deep monte carlo tree search. *IEEE Transactions on Vehicular Technology*, 69(7):7146–7158, 2020.
- [6] Y.-Q. Chen, Y. Chen, C.-K. Lee, S. Zhang, and C.-Y. Hsieh. Optimizing quantum annealing schedules with monte carlo tree search enhanced with neural networks. *Nature Machine Intelligence*, 4(3):269–278, 2022.
- [7] S. Chetlur, C. Woolley, P. Vandermersch, J. Cohen, J. Tran, B. Catanzaro, and E. Shelhamer. cudnn: Efficient primitives for deep learning, 2014.
- [8] F. Chollet et al. Keras. <https://keras.io>, 2015.
- [9] H. Deng, X. Yuan, Y. Tian, and J. Hu. Neural-augmented two-stage monte carlo tree search with over-sampling for protein folding in hp model. *IEEJ Transactions on Electrical and Electronic Engineering*, 17(5):685–694, 2022.
- [10] C. Gao, R. Hayward, and M. Müller. Move prediction using deep convolutional neural networks in hex. *IEEE Transactions on Games*, 10(4):336–343, 2018.

- [11] J. Ghorpade, J. Parande, M. Kulkarni, and A. Bawaskar. Gpgpu processing in cuda architecture. *Advanced Computing: An International Journal*, 3(1):105, Jan 2012.
- [12] I. J. Goodfellow, Y. Bengio, and A. Courville. *Deep Learning*. MIT Press, Cambridge, MA, USA, 2016.
- [13] C. Guo, G. Pleiss, Y. Sun, and K. Q. Weinberger. On calibration of modern neural networks. In D. Precup and Y. W. Teh, editors, *Proceedings of the 34th International Conference on Machine Learning*, volume 70 of *Proceedings of Machine Learning Research*, pages 1321–1330. PMLR, 06–11 Aug 2017.
- [14] T. Ha, K. Cho, G. Cha, K. Lee, and S. Oh. Vehicle control with prediction model based monte-carlo tree search. In *17th International Conference on Ubiquitous Robots (UR)*, pages 303–308, 2020.
- [15] I. Karafyllis, D. Theodosis, and M. Papageorgiou. Two-dimensional cruise control of autonomous vehicles on lane-free roads. *arXiv preprint arXiv:2103.12205*, Mar 2021.
- [16] A. Karalakou, D. Troullinos, G. Chalkiadakis, and M. Papageorgiou. Deep reinforcement learning reward function design for autonomous driving in lane-free traffic. *Systems*, 11(3), 2023.
- [17] T. Kavzoglu. Increasing the accuracy of neural network classification using refined training data. *ResearchGate*, 2009.
- [18] M. Kemmerling, D. Lütticke, and R. H. Schmitt. Beyond games: a systematic review of neural monte carlo tree search applications. *Applied Intelligence*, 54(1):1020–1046, 2024.
- [19] B. Kim, K. Lee, S. Lim, L. Kaelbling, and T. Lozano-Perez. Monte carlo tree search in continuous spaces using voronoi optimistic optimization with regret bounds. *Proceedings of the AAAI Conference on Artificial Intelligence*, 34(06):9916–9924, Apr. 2020.
- [20] L. Kocsis and C. Szepesvári. Bandit based monte-carlo planning. In *Machine Learning: ECML 2006*, pages 282–293, Berlin, Heidelberg, 2006. Springer Berlin Heidelberg.
- [21] J. Lee, W. Jeon, G.-H. Kim, and K.-E. Kim. Monte-carlo tree search in continuous action spaces with value gradients. *Proceedings of the AAAI Conference on Artificial Intelligence*, 34(04):4561–4568, Apr. 2020.
- [22] L. Lei, R. Luo, R. Zheng, J. Wang, J. Zhang, C. Qiu, L. Ma, L. Jin, P. Zhang, and J. Chen. Kb-tree: Learnable and continuous monte-carlo tree search for autonomous driving planning. In *2021 IEEE/RSJ International Conference on Intelligent Robots and Systems (IROS)*, pages 4493–4500, Prague, Czech Republic, 2021. IEEE Press.
- [23] J. Moon, J. Kim, Y. Shin, and S. Hwang. Confidence-aware learning for deep neural networks. *arXiv preprint arXiv:2007.01458*, 2020.
- [24] M. Papageorgiou, K.-S. Mountakis, I. Karafyllis, I. Papamichail, and Y. Wang. Lane-free artificial-fluid concept for vehicular traffic. *Proceedings of the IEEE*, 109(2):114–121, 2021.
- [25] A. Rincioig, C. Mieth, P. M. Scheikl, and A. Meyer. Sheet-metal production scheduling using alphago zero. In *Proceedings of the Conference on Production Systems and Logistics: CPSL 2020*, Hannover, Germany, 2020. Leibniz Universität Hannover.

- [26] S. Rodriguez and P. Cardiff. A general approach for running python codes in openfoam using an embedded pybind11 python interpreter. *arXiv preprint arXiv:2203.16394*, 2022. Preprint submitted to OpenFOAM Journal.
- [27] D. Silver, T. Hubert, J. Schrittwieser, I. Antonoglou, M. Lai, A. Guez, M. Lanctot, L. Sifre, D. Kumaran, T. Graepel, T. Lillicrap, K. Simonyan, and D. Hassabis. A general reinforcement learning algorithm that masters chess, shogi, and go through self-play. *Science*, 362(6419):1140–1144, 2018.
- [28] S. Song, H. Chen, H. Sun, and M. Liu. Data efficient reinforcement learning for integrated lateral planning and control in automated parking system. *Sensors*, 20(24), 2020.
- [29] M. Świechowski, K. Godlewski, B. Sawicki, and J. Mańdziuk. Monte carlo tree search: a review of recent modifications and applications. *Artificial Intelligence Review*, Jul 2022. Published online.
- [30] D. Troullinos, G. Chalkiadakis, D. Manolis, I. Papamichail, and M. Papageorgiou. Extending sumo for lane-free microscopic simulation of connected and automated vehicles. In *SUMO Conference Proceedings*, volume 3, pages 95–103, Sep 2022.
- [31] D. Troullinos, G. Chalkiadakis, I. Papamichail, and M. Papageorgiou. Collaborative multi-agent decision making for lane-free autonomous driving. In *AAMAS '21*, pages 1335–1343, Virtual Event, United Kingdom, 2021. International Foundation for Autonomous Agents and Multiagent Systems.
- [32] V. K. Yanumula, P. Typaldos, D. Troullinos, M. Malekzadeh, I. Papamichail, and M. Papageorgiou. Optimal trajectory planning for connected and automated vehicles in lane-free traffic with vehicle nudging. *IEEE Transactions on Intelligent Vehicles*, 8(3):2385–2399, 2023.
- [33] T. Yee, V. Lisỳ, M. H. Bowling, and S. Kambhampati. Monte carlo tree search in continuous action spaces with execution uncertainty. In *IJCAI*, pages 690–697, 2016.

Appendix

A Probabilistic Learning and Calibration in Neural Networks

In a supervised learning problem, accuracy [17] measures the percentage of correct predictions, while confidence [23] indicates the probability that a given prediction is correct, providing insight into the reliability of individual predictions.

Learning from probabilistic data involves handling situations where the same input can lead to different outcomes with certain probabilities. In stochastic processes and probabilistic scenarios (like MCTS), traditional accuracy metrics can be misleading, as they may unfairly penalize the model for making reasonable predictions that do not align perfectly with the true labels due to inherent data uncertainty. This necessitates the use of alternative metrics to evaluate model performance more accurately.

Model calibration [13] is used to evaluate a neural network (NN)’s output probabilities, ensuring they accurately reflect true outcome probabilities. This evaluation ensures that the predicted confidence level \hat{P} aligns with the actual likelihood of correctness. Ideal calibration is expressed mathematically as $P(\hat{Y} = Y | \hat{P} = p) = p$ for all p in the range $[0, 1]$. Achieving it is challenging, especially in a multiclass setting, due to the continuous nature of the probability variable.

Reliability diagrams [13] visualize model calibration by plotting predicted confidence against actual accuracy. Predictions are divided into M equally sized bins based on confidence scores, representing the range $(\frac{m-1}{M}, \frac{m}{M}]$. Actual accuracy for each bin B_m is calculated as: $\text{acc}(B_m) = \frac{1}{|B_m|} \sum_{i \in B_m} 1(\hat{y}_i = y_i)$, where \hat{y}_i and y_i are the predicted and true labels. Average confidence for each bin is: $\text{conf}(B_m) = \frac{1}{|B_m|} \sum_{i \in B_m} \hat{p}_i$, where \hat{p}_i is the confidence level for each prediction.

Perfect calibration occurs when accuracy equals average confidence in each bin. Confidence histograms [13] complement reliability diagrams by showing the distribution and number of samples across confidence bins, providing a visual summary of prediction confidences across the dataset.

A.1 Data Collection and Pre-training

Continuing with the integration process of the NN to MCTS, we must first gather our dataset for training the network. To construct the NN for learning purposes, we collect data through self-play simulations using the plain MCTS (nudging) algorithm at 1000 iterations for high quality solutions. This dataset includes inputs (states) and corresponding labels (best actions determined by MCTS). Each input state consists of specific attributes:

Ego vehicle values: Characterized by parameters $\{p_y, u_x, u_y, w, l, d_u\}$ (6 values); excluding the x position (p_x), as it does not influence the decision-making process.

Neighbor vehicle values: Account for the 4 nearest vehicles in front and the 4 behind within a 50-meter visibility range, defined by parameters $\{dx, dy, u_x, u_y, w, l, d_u\}$ for each vehicle, (total 56 values). The values dx and dy are the distances in positions longitudinal and lateral relative to the ego vehicle.

If there are more than 4 vehicles either in front or behind, the closest ones are prioritized. If fewer than 4 vehicles are present, “virtual” neighbors with predefined parameters ;so the NN can distinguish them from real neighbors; are introduced, ensuring the state vector’s completeness. The final dataset consists of 63 elements: 62 values represent a state, and 1 value denotes the best action.

A.2 Training and Accuracy

After generating our dataset, we created and trained our NN classifier to predict the most likely action given a state from the SUMO simulation. Despite optimization and fine-tuning, the NN's accuracy only reached 72%. This raised concerns about the network's learning capability.

The inherent probabilistic nature of MCTS data, due to random actions rollouts in simulation phase, resulted in identical states leading to different best actions. The NN, however, simplifies this by predicting the most probable action, producing a deterministic policy. This discrepancy explains the low accuracy. To ensure our NN is functioning correctly and learning effectively from the data, we validate its performance with the use of reliability diagrams that reflect the probabilistic nature of the learned policy.

A.3 Reliability Diagrams for Neural Network Evaluation

To evaluate our model's calibration, we divided the dataset into 10 bins based on the probability of the most probable prediction for each sample, ranging from $[0, 0.1]$ up to $[0.9, 1]$. We calculated the actual confidence and accuracy for each bin, aiming for the ideal where confidence equals accuracy.

A.3.1 Reliability Diagram

We used reliability diagrams to visualize our model's calibration against the perfect calibration line. As shown in figure below, our model closely aligns with the ideal calibration line, indicating it is well-calibrated.

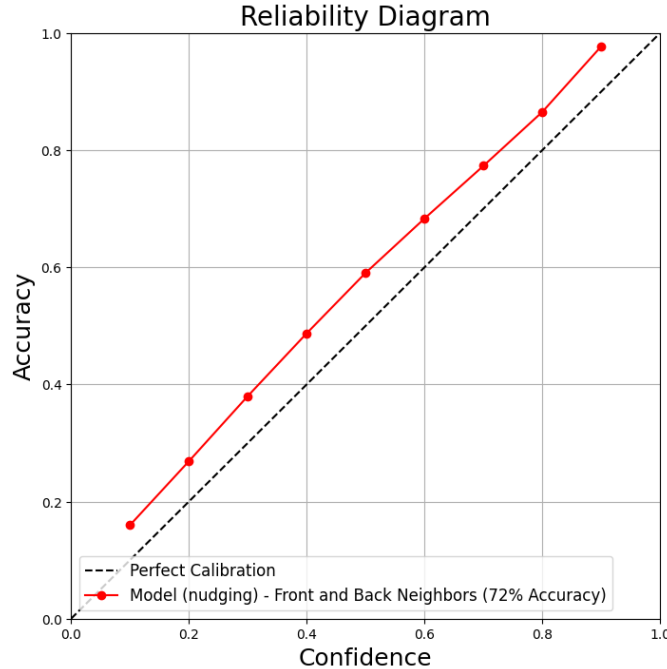


Figure 15: Reliability Diagram - Model's Calibration and Perfect Calibration.

A.3.2 Confidence Histogram

Additionally, we created a histogram of confidence to show the distribution of sample predictions across the bins. From figure below, we understand that the samples are distributed correctly, starting from zero and gradually increasing in each next bin. This indicates fewer predictions with low confidence and a proper distribution of prediction confidence levels.

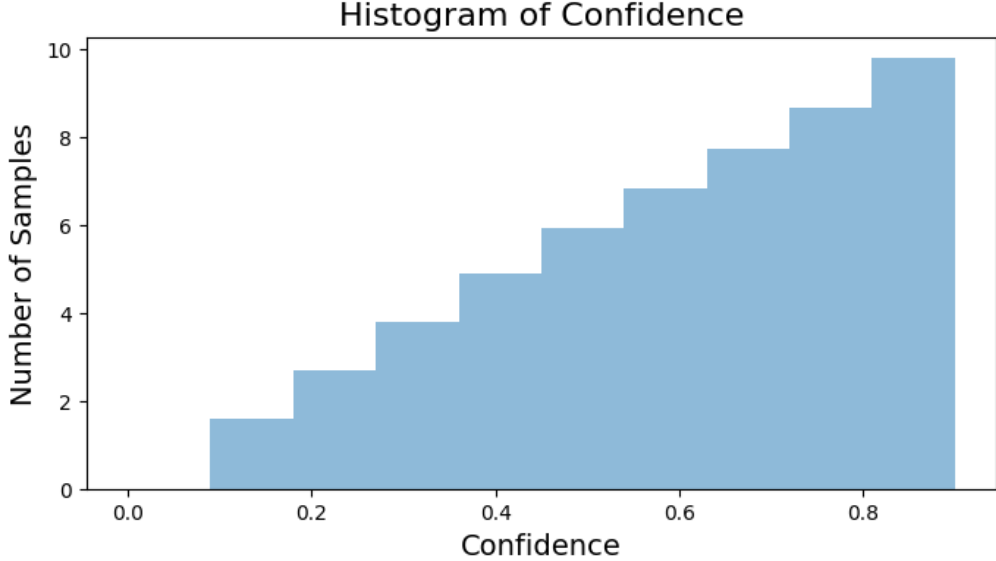


Figure 16: Histogram of Confidence - Number of Samples per Bin.

Finally, another evidence of our network’s learning capability and performance is observed when we eliminate the inherent randomness of the MCTS algorithm. By setting the maximum rollout state depth to 1 (from its current value of 6), making the next state always deterministic, our NN trained with this data achieved an accuracy of 95.8%. This significantly higher accuracy strongly supports our assertion.

B Time overhead of NN Predictions

In this section we detail how our NN produces its predictions $P(s, a)$ and the gradual process of refining the functionality and speed of our algorithm.

B.1 Single Predictions in Current State

Initially, our process involved generating predictions for each state in MCTS run-time. The predictive function took the current state and returned a probability distribution of 15 possible actions. This output was then used in the MCTS’s selection phase to determine the best action.

B.2 Inefficiencies and Speed Improvements

The initial approach was slow because it repeatedly calculated predictions from start for each selection phase, leading to many redundant calculations. To address this, we stored predic-

tions after the first visit to each node (memoization). When revisiting a state, the algorithm retrieved the stored predictions, significantly reducing redundant computations and speeding up the process.

Further optimization focused on transitioning from single to batch predictions. Initially, each prediction call involved overhead from repeatedly invoking a Python script from MCTS run-time which has been written in C++. By adopting batch processing, we utilized the NN’s capability to process multiple inputs simultaneously. This change minimized script call overhead and maximized computational efficiency, resulting in a faster, more streamlined algorithm.

B.3 Batch Predictions in Child Expansion

Our strategy for implementing batch predictions involved generating predictions in batches of 15, corresponding to each potential child action of a node. When expanding a node, we computed the predictions for its 15 potential child states and stored each prediction within the respective child nodes. This approach ensured that when revisiting any of these child states, we could directly use the previously calculated predictions, eliminating the need for recalculations. An exception to this method was the root node, which required a single prediction to determine its initial set of predictions.

In terms of speed improvement, shifting to batch processing for 15 predictions at once resulted in significant efficiency gains. The average time required for a single prediction was 13 times faster compared to making 15 individual predictions.

C Algorithm Implementation

C.1 Navigation in Autonomous Driving Decision Space

To construct the MCTS tree for our autonomous driving environment, nodes represent specific states s . Starting from the current state as the root node, each node is connected by edges that represent actions, defined as pairs of longitudinal and lateral accelerations. From any given state, there are 15 possible actions, resulting in 15 child nodes. When a new action is taken, it transitions from the current state to a new one. During the simulation phase, the value for each state is calculated using the reward function $r(s)$. This value is then backpropagated through the tree, updating the average reward of each state accordingly.

C.2 NN Predictions

C.2.1 Batch Predictions in Algorithm’s Start

To enhance the speed of our predictions, we transitioned from generating small batches to calculating predictions for the entire MCTS state space in one go, storing them in an external predictions matrix. This method maximizes the NN batch processing capabilities and eliminates prediction calculations during run-time. Initially, we construct the complete tree state space up to a predefined maximum depth, typically depth 3, based on experimental observations that deeper states are rarely visited for expansion, thus there is no need for calculating their predictions.

C.2.2 Optimizing Predictions Storage and Retrieval

By generating predictions for the entire tree in one batch and storing them in a matrix, we significantly reduce the time needed for predictions. When the algorithm runs, it retrieves

the necessary predictions from this matrix, just by one memory access, bypassing the need for repeated calculations. This approach ensures that we make the script call only once before the MCTS algorithm starts running, leveraging the efficiency of batch processing. Although the batch processing method involves pre-calculating predictions for states that might not be visited, thus they are redundant, the overall performance enhancement makes this trade-off acceptable. In Algorithm 1, we provide a high level implementation of the NN-Guided MCTS algorithm and the selection function it employs (Algorithm 2).

Algorithm 1: A High Level Pseudocode of NN-Guided MCTS

Input: *current state*
model \leftarrow load trained neural network once ()
iterations \leftarrow 0
root \leftarrow initialize tree (*current state*)
predictions \leftarrow batch predictions (*model, data tree*)
while *iterations* \leq MAX ITERATIONS **do**
 if *state depth* \leq MAX DEPTH **then**
 | *state prediction* \leftarrow *predictions* [*state index*]
 | *selected state* \leftarrow select(*root, state prediction*)
 end
 else
 | *state prediction* \leftarrow single prediction (*model, data single*)
 | *selected state* \leftarrow select (*root, state prediction*)
 end
 if *is terminal* (*selected state*) **then**
 | **continue**
 end
 expanded state \leftarrow expand (*selected state*)
 score \leftarrow simulate (*expanded state*)
 backpropagate (*expanded state, score*)
 iterations \leftarrow *iterations* + 1
end
return *best action*

Algorithm 2: Selection Phase of NN-Guided MCTS

Input: *state, prediction*
children \leftarrow get children (*state*)
for *child* \in *children* **do**
 | *score* \leftarrow PUCT (*state, child, prediction*)
end
bestchild \leftarrow $\text{argmax}_{\text{child}}$ (*score*)
return *best child*

C.2.3 Speed Improvement

This refined approach led to significant speed improvements. The batch prediction method is 10.2 times faster than the previous 15-batch approach and 132.6 times faster than the original

Predictions	Batch Size	Tree Depth	Time needed in (ms)
1		1	26
16		2	30
241		3	44
3616		4	182

Table 3: Time in milliseconds needed for varying Predictions Batches.

single prediction method. By pre-calculating predictions and storing them in a matrix, we avoid runtime calculations, streamlining the entire process and achieving substantial performance gains. In Table 3 we can see detailed time metrics for each batch of predictions.

C.2.4 Decision on Tree Depth

We observed experimentally that our state space tree, after passing depth 3 tends to explore states mostly in width and not so much in depth. This means, that almost always it reached only up to depth 4 and very rarely depth 5. This remained the case not only when operating with few iterations, but also when it was tested with high number of iterations, thus more time to explore in depth if it had been more beneficial. So we concluded that we always need the predictions for states in depth 3, so we can expand to depth 4, but we do not need predictions for depth 4 to go to 5. Therefore, we empirically determined that creating our predictions tree up to depth 3 was the most favourable, as further depths resulted in exponentially increased states and computational time without proportional benefits. For example, depth 3 has 241 states, while depth 4 jumps to 3616 states. Hence, depth 3 balances computational efficiency and prediction accuracy. During runtime, if the current state’s depth exceeds this predefined depth, a single prediction is made for that state, ensuring that all necessary predictions are available.

C.3 Deep Neural Network without Search

In this section, we consider a simple alternative that uses the NN in a greedy manner without any underlying search mechanism like MCTS. At each state, the algorithm makes a single prediction and selects the action with the highest probability. This straightforward approach, while potentially less effective due to its lack of strategic depth, serves as a useful benchmark. By comparing its performance against traditional MCTS and NN-guided MCTS, we can better understand the benefits and limitations of relying solely on NN knowledge for decision-making.

C.4 Agent and Hyper-parameter Setup

In this section, we outline the key parameters and technical elements relevant to our agent and the MCTS algorithm. The development of the NN was facilitated by Tensorflow-Keras [1, 8] for batch processing acceleration using CUDA [11] and cudnn [7]. Integration into the MCTS framework which was implemented in C++, was achieved through Pybind11 [26], allowing Python scripts to run during C++ runtime. Tables 4, 5, 6 below provide detailed information on the NN architecture, MCTS algorithm parameters and training parameters respectively.

D Additional Results

In Tables 7, 8, 9, we provide the exact numerical results regarding collisions associated with the figures in the main paper. Then, in Table 10, we include the collision results for the NN-only

Parameter	Value
Input Layer	62 (one MCTS state)
Hidden Layers	512, (0.3 dropout), 256, (0.3 dropout), 128
Output Layer	15 (MCTS possible actions)
Type	Feed Forward
Activation Function	ReLU (hidden layers), Softmax (output layer)
Optimizer	Adam
Batch Size	64
Epochs	50
Learning Rate	start 0.001 and descending
Accuracy	72% (rollout depth 6) , 95.8% (rollout depth 1)
Front Neighbors (dataset)	4
Back Neighbors (dataset)	4
Visibility Target (m)	50

Table 4: NN Architecture and Training Parameters.

Parameter	Value
D	10
ϵ	1
Min Visits	5
Max Rollout Depth	6
Lateral Actions	-1, 0, 1
Longitudinal Actions	-5, -2, 0 , 2, 5

Table 5: MCTS Parameters.

Parameter	Value
CPU	Ryzen 5 3600
RAM	16 GB
GPU	RTX 3060 4GB
OS	Windows 10
cudnn capability	8.6
Python Version	3.10.8
Tensorflow Version	2.9.1

Table 6: Technical specifications and versions for utilized packages.

variant.

NN-MCTS	MCTS (nudging)	MCTS	Iterations
0	0	3.8 ± 0.84	1000
0	0	3.8 ± 0.84	750
0	0	3.8 ± 0.84	500
0	2.6 ± 0.9	7 ± 3.39	200
0	7.6 ± 3.4	12.6 ± 4.77	100
29.8 ± 3.9	27.4 ± 6.3	29.2 ± 9.04	50
113.8 ± 16.2	90 ± 14.6	92.8 ± 18.28	30

Table 7: Comparative Results of Collisions \pm SD for NN-MCTS, MCTS (nudging), and MCTS across different Iterations for 5400 *veh/h*.

NN-MCTS	MCTS (nudging)	MCTS	Iterations
0	0	25.8 ± 4.92	1000
0	0	35.2 ± 5.54	750
0	0	48.6 ± 9.37	500
0	4.6 ± 1.82	55 ± 11.47	200
6.4 ± 1.52	11 ± 5.52	72 ± 19.07	100
44.2 ± 7.09	39.4 ± 12.3	98.8 ± 21.1	50
120.8 ± 19.43	112.4 ± 21.33	125.2 ± 27.93	30

Table 8: Comparative Results of Collisions±SD for NN-MCTS, MCTS (nudging), MCTS across different Iterations for 9400 *veh/h*.

NN-MCTS	MCTS (nudging)	MCTS	Iterations
0	0	-	1000
0	0	-	750
0	0	-	500
0	9.2 ± 2.58	-	200
10.4 ± 2.6	16.8 ± 5.4	-	100
95.4 ± 23.1	63.6 ± 16.21	-	50
400.8 ± 37.29	384.8 ± 48.33	-	30

Table 9: Comparative Results of Collisions±SD for NN-Guided MCTS, MCTS (nudging), and MCTS across different Iterations for 12000 *veh/h*.

5400 veh.flow/h.	9400 veh.flow/h.	12000 veh.flow/h.
22	35	61

Table 10: NN Collisions for each flow demand *veh/h*.

With regards to speed, the numerical results can be found in Table 11. There, the calculated standard deviation (SD) values were consistently close to 0 and therefore we omitted their report.

An additional metric to evaluate our methods is delay, which measures the difference between actual travel time and ideal travel time based on desired speeds, with lower values indicating better policies, where more vehicles better follow their desired speed objective. In Figures 17–19 and Table 12, we report on these results across all the methods. There, we have consistent findings, again that isotropic state information improves upon delay times (due to nudging), and the NN positively impacts the solution quality especially after a certain number of iteration. As in the speed related results, we observed very small SD values across all variants.

veh/h	NN-Guided MCTS	MCTS (nudging)	MCTS	NN
5400	28.75	28.67	28.4	28.42
9400	28	27.92	26.94	27.61
12000	27.5	27.41	-	26.98

Table 11: Speed Average in m/s for NN-Guided MCTS, MCTS (nudging), MCTS and NN for different Vehicle Flows.

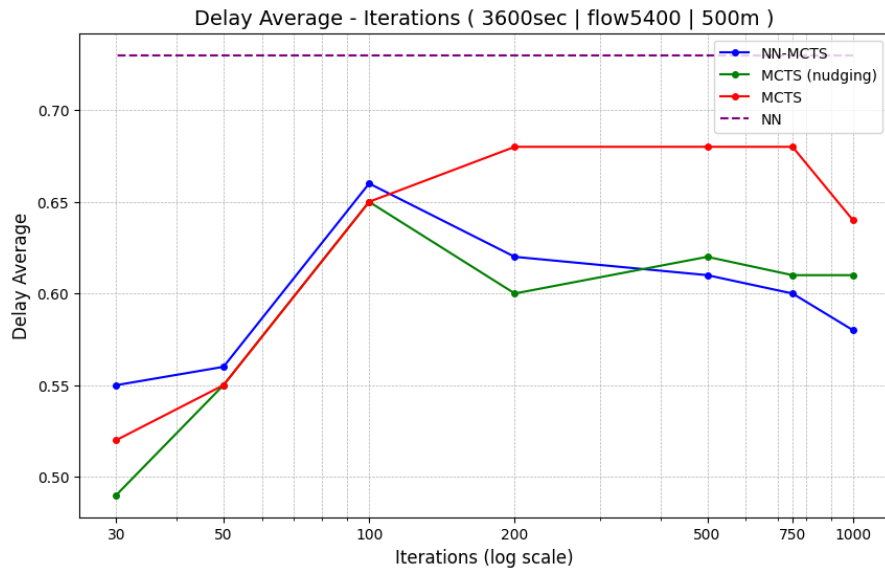


Figure 17: Delay Average \pm SD for NN-MCTS, MCTS (nudging), MCTS and NN across different iterations for 5400 *veh/h*.

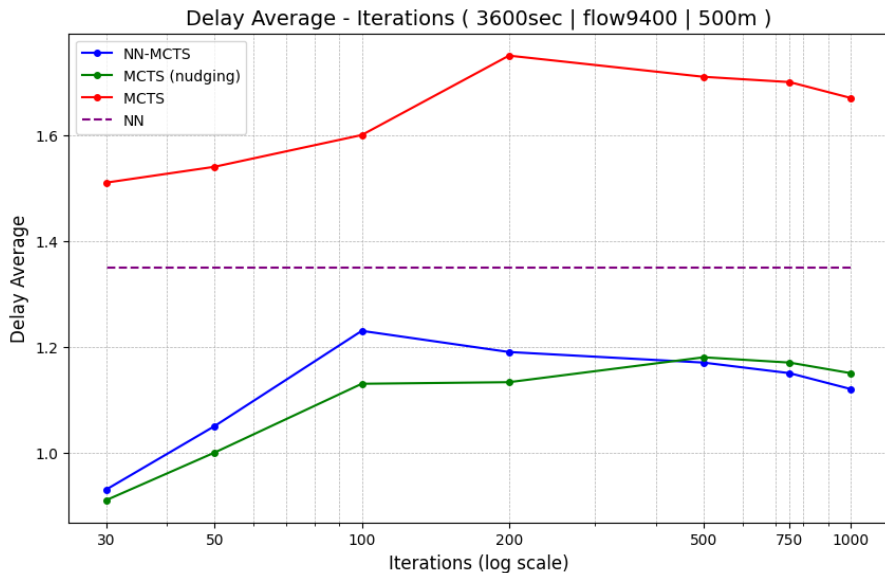


Figure 18: Delay Average \pm SD for NN-MCTS, MCTS (nudging), MCTS and NN across different iterations for 9400 *veh/h*.

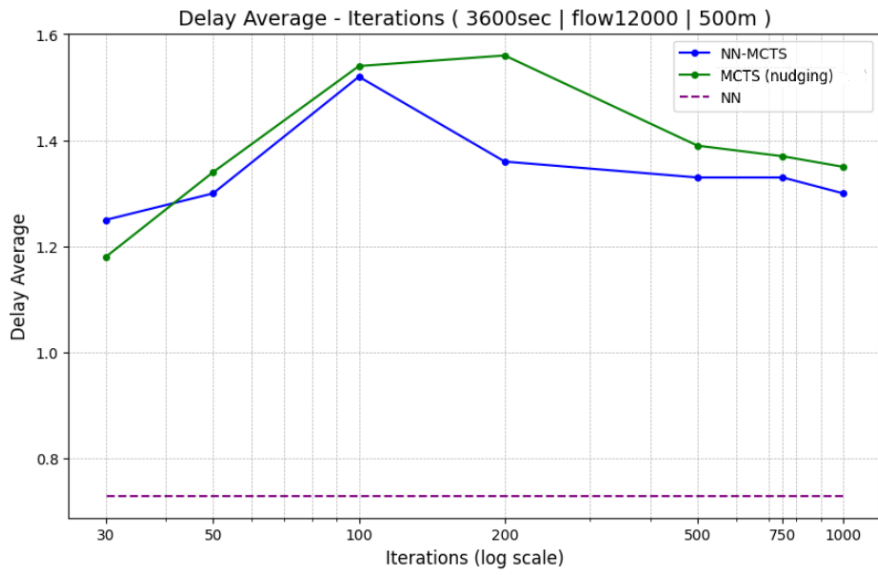


Figure 19: Delay Average \pm SD for NN-MCTS, MCTS (nudging), MCTS and NN across different iterations for 12000 veh/h .

veh/h	NN-Guided MCTS	MCTS (nudging)	MCTS	NN
5400	0.58	0.61	0.64	0.73
9400	1.12	1.15	1.67	1.35
12000	1.3	1.35	-	1.69

Table 12: Delay Average in ms for NN-Guided MCTS, MCTS (nudging), MCTS and NN for different vehicle flows.